Seismic monitoring on a piled raft combined with grid-form deep mixing walls in soft ground

Kiyoshi Yamashita[1] and T. Tanikawa[1]

[1] R&D Institute, TAKENAKA Corporation, 5-1,1Chome, Ohtsuka, Inzai, Chiba, 270-1395, Japan.

ABSTRACT

The seismic behavior of a piled raft with grid-form deep mixing walls (DMWs) in soft ground was investigated using the observation records of the 2011 Tohoku Earthquake (M_w=9.0), focusing the inertial and kinematic effects from the structure and the ground movement on the foundation system. It was found that the bending moments near the pile head are affected mainly by the ground deformation rather than the shear force resulted from the inertial force, even though the amplification of the ground deformation below the raft was restrained by the DMWs.

Keywords: piled raft; soft ground; deep mixing; grid type; seismic monitoring; the 2011 Tohoku Earthquake

1 INTRODUCTION

The effectiveness of piled rafts in reducing overall and differential settlements has been confirmed not only in favorable ground conditions but also in unfavorable ground conditions, as reported by many researchers. Recently, it has been also recognized that piled rafts could be resilient against seismic events. However, case histories on monitoring seismic soil-pile-structure interaction of full-scale piled rafts are very limited. This paper presents seismic behavior of a piled raft foundation with DMWs supporting a 12-story building based on the records of the 2011 Tohoku Earthquake (Yamashita et al., 2012), focusing on the inertial and kinematic effects from the structure and the ground movement on the pile bending moment.

2 BUILDING AND SOIL CONDITIONS

Fig. 1 shows a schematic view of the building and the foundation with a typical soil profile. The building located in Tokyo is a reinforced concrete structure with a seismic base isolation system and the total load was 198.8 MN. To improve the bearing capacity of the soft silty clay beneath the raft, as well as to cope with the liquefiable silty sand just below the raft, the grid-form DMWs were constructed to a depth of 16 m with the bottom being embedded in the stiffer silty clay. Sixteen 45-m-long piles were used. Fig. 2 shows the layout of the piles and the grid-form DMWs. Two piles, 5B and 7B, were provided with a couple of LVDT-type strain gauges. A vertical array consisting of borehole-type

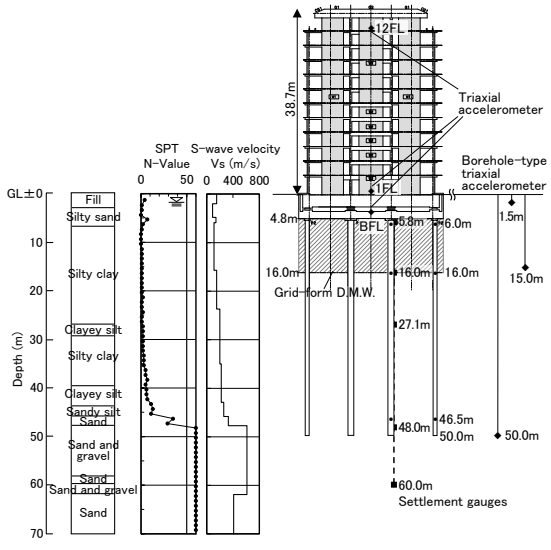

Fig. 1. Schematic view of building and foundation with soil profile.

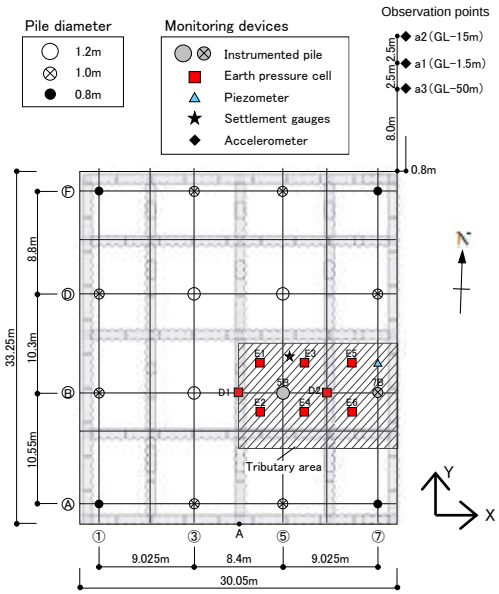

Fig. 2. Layout of piles and grid-form deep mixing walls with locations of monitoring devices.

triaxial servo accelerometers was installed at three depths. Further details of the foundation design and the field monitoring have been described by Yamashita et al. (2012).

3 SEISMIC MONITORING RESULTS

Fig. 3 shows the acceleration histories of the ground and the structure in the EW direction. A peak horizontal ground acceleration of 1.75 m/s^2 was observed near the ground surface. Fig. 4 shows the Fourier spectra of the EW acceleralations of the ground and structure response. The predominant period of the ground near the surface (T_g) was around 1 s. It should be noted that the natural period of the base isolation system (T_b) is 3.5 s for moderate earthquake motions, while the fixed based natural period of the superstructure is 0.96 s.

Fig. 5 shows the time histories of the ground displacement near the surface (at 1.5 m depth) and the raft displacement (denoted δS and δR, respectively), including the maximum and minimum responses. The displacements, which are relative values to that at 50 m depth, were calculated by the double integration of the acceleration records. It is seen that the amplitude of δS was greater than that of δR, which occurred because T_g of the soft clay deposit was fairly long. The time history of the ground displacement at 15 m depth is also shown in Fig. 5. All the displacement histories were in phase. Fig. 6 shows the relations of the displacement of the ground at 15 m depth with δS and δR. It is seen that the ground displacement at 1.5 m depth was significantly amplified from that at 15 m depth. On the other hand, the raft displacement was almost identical to the ground displacement near the surface. This means that the amplification of the ground displacements under the raft was kinematically restrained by the grid-form DMWs.

Fig. 7 shows the time histories of the bending moments near the pile head (at 6 m depth) and at 16 m depth in Pile 5B in the EW direction. The peaks of the bending moment near the pile head were greater than those at 16 m depth. The maximum and minimum bending moments were generated at t=109.08 s and t=108.51 s (referred as t_{Mmax} and t_{Mmin}, respectively).

4 INERTIAL AND KINEMATIC EFFECTS ON PILE MOMENT

Fig. 8 shows the relations of δS with the bending moment near the pile head in Pile 5B. The bending moment near the pile head increased with the increase in ground displacement and had strong correlation with the ground displacement near the surface.

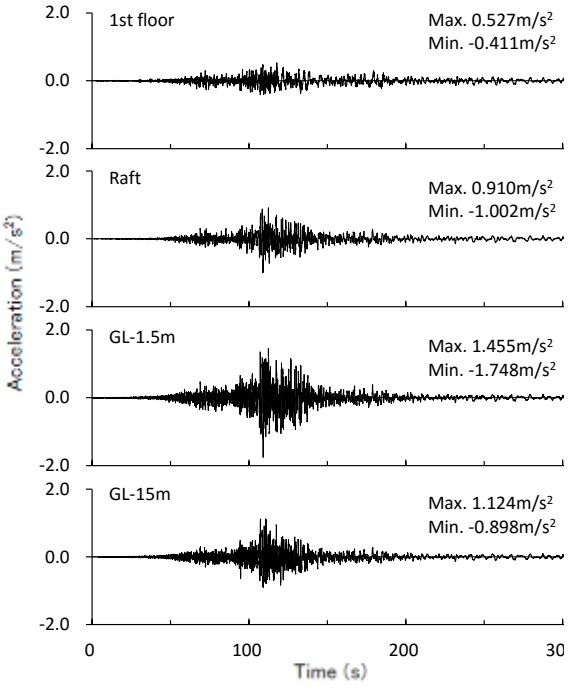

Fig. 3. Accelerations histories of ground and structure (EW).

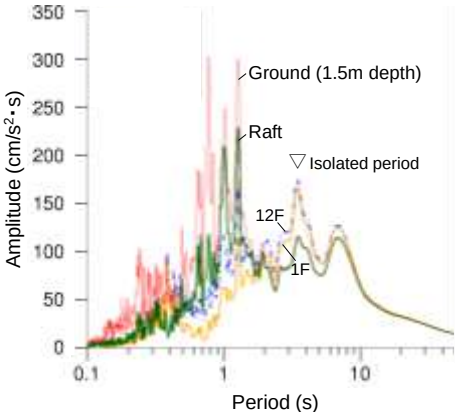

Fig. 4. Fourier spectra of accelerations of ground and structure response (EW).

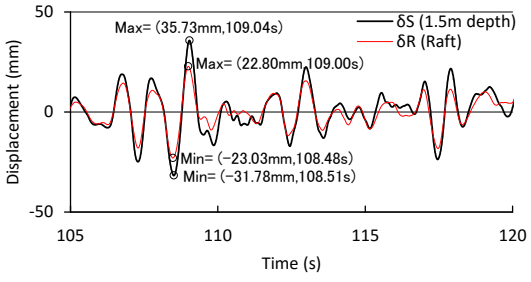

(a) δS and δR

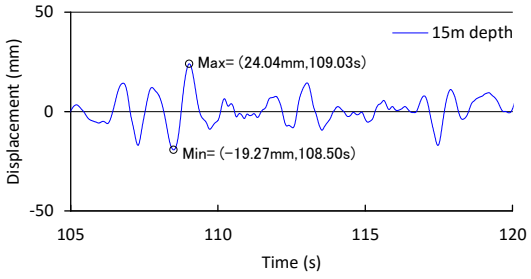

(b) Ground at 15m

Fig. 5. Displacement histories of ground and raft (EW).

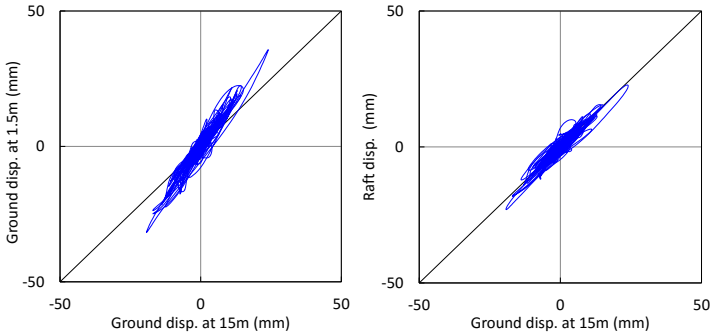

(a) Ground at 15m vs. δ*S* (b) Ground at 15m vs. δ*R*

Fig. 6. Relations of ground displacement at 15m depth with δ*S* and δ*R* (EW).

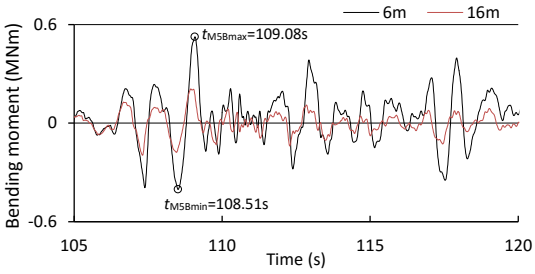

Fig. 7. Time histories of bending moment in Pile 5B (EW).

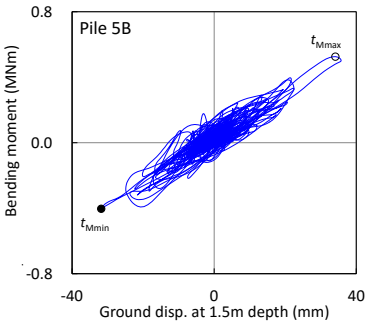

Fig. 8. δ*S* vs. bending moment near pile head in Pile 5B (EW).

Fig. 9 shows the time history of inertial forces which are superstructure inertial force, raft inertial force and the sum of the superstructure and raft inertial forces (referred as structure inertial force). The inertial forces can be estimated using the mass in structural design (1.55×10^7 kg for the superstructure and 4.18×10^6 kg for the raft) and the accelerations recorded on the raft, the first and twelfth floors (Hamada et al., 2014). It is seen that the peaks of the superstructure inertial force were slightly greater than those of the raft inertial force due to the action of the base isolation system. Fig. 10 shows the relation of the raft inertial force with the superstructure inertial force. There appears to be no or somewhat negative correlation between them. Hence, the peaks of the structure inertial force were comparable with those of the superstructure inertial force, as is seen in Fig. 9.

Fig. 11 shows the relations of the inertial force with the bending moment near the pile head in Pile 5B. The bending moment had strong correlation with the raft inertial force. This arises because the raft is embedded in the ground, and the raft inertial force may have a significant correlation with the ground displacement (which had strong correlation with the bending moment). In contrast, the bending moment had almost no correlation with the superstructure inertial force due to the phase difference between the superstructure and the raft, as shown in Fig. 10.

Fig. 12 shows the relation of the relative displacement (δ*S*-δ*R*) with the bending moment near the pile head in Pile 5B. According to Tamura and Hida (2014), the dynamic earth pressure acting on the raft side, which means the resultant force of the earth pressure (the sum of the active and passive earth pressure) and the side friction, would increase with the increase in the relative displacement. Hence, Fig. 12 suggests that the bending moment near the pile head had significant correlation with the dynamic earth pressure.

Fig. 13 illustrates a schematic of the inertial forces and the ground displacements near the surface generated at t_{Mmax} and t_{Mmin}, where α_1: a ratio of the ground displacement near the surface to its maximum or minimum, α_2; a ratio of the relative displacement

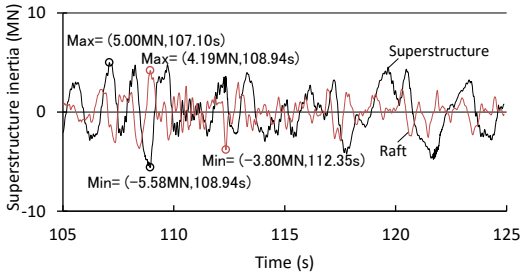

(a) Superstructure and raft inertial forces

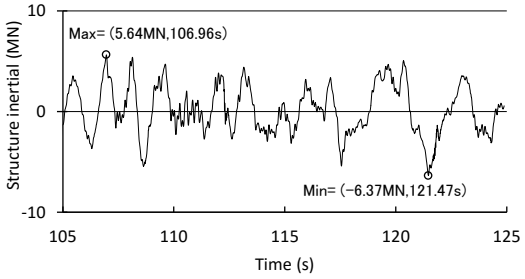

(b) Structure inertial force

Fig. 9. Time histories of inertial forces (EW).

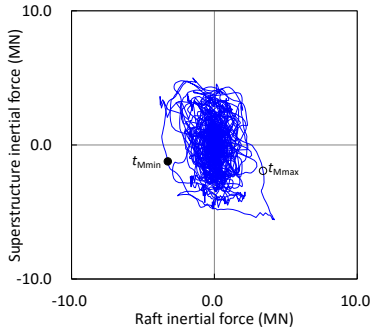

Fig. 10. Raft inertial force vs. superstructure inertial force (EW).

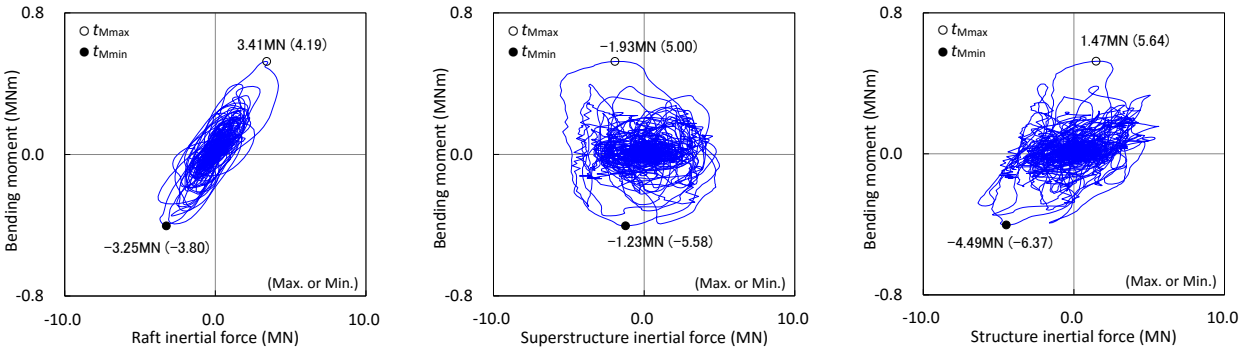

(a) Raft inertial force (b) Superstructure inertial force (c) Structure inertial force

Fig. 11. Inertial force vs. bending moment near pile head in Pile 5B (EW).

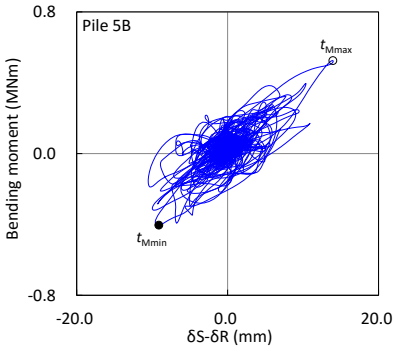

Fig. 12. (δS-δR) vs. bending moment near pile head (EW).

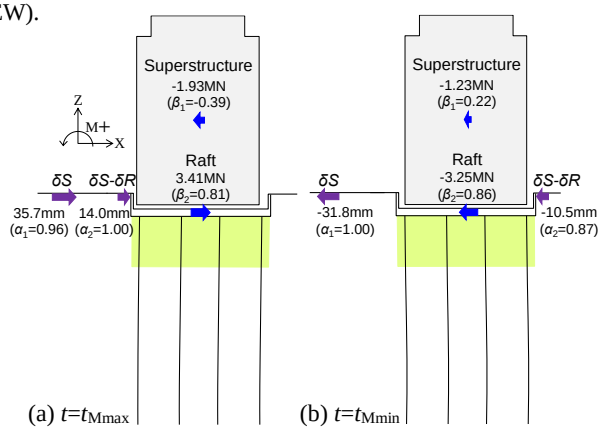

(a) t=t_{Mmax} (b) t=t_{Mmin}

Fig. 13. Inertial forces and ground displacements generated at t_{Mmax} and t_{Mmin} (EW).

(δS-δR) to its maximum or minimum, β_1; a ratio of the superstructure inertial force to its maximum or minimum, β_2; a ratio of the raft inertial force to its maximum or minimum, β; a ratio of the structural force to its maximum or minimum. The values of α_1, α_2, β_1, β_2 and β were obtained from Figs. 8, 11 and 12. The values of α_1, α_2 and β_2 were greater than 0.8, i.e., the ground displacement, the relative displacement and the raft inertial force were close to their maximum or minimum when the bending moment was at its maximum or minimum, respectively. On the other hand, the values of β_1 were -0.39 at t_{Mmax} and 0.22 at t_{Mmin}, i.e., the superstructure inertial force was out of phase with the raft inertial force or a small part of its minimum was generated at that time. Additionally, the values of β were 0.26 at t_{Mmax} and 0.70 at t_{Mmin}. These results are consistent with the experimental and analytical simulation results reported by Tamura et al. (2012) when T_b is longer than T_g.

Thus, the kinematic effects arising from the ground displacement, which significantly affect the raft inertial force and the dynamic earth pressure acting on the raft side, on the maximum bending moment was dominant over the inertial effects from the superstructure. In such a case, the restraint on the ground displacement by the DMWs could decrease the bending moment of the piles significantly (Yamashita et al, 2018).

5 CONCLUDING REMARKS

The seismic monitoring results have shown that the maximum bending moments of the piles were affected mainly by the kinematic effects arising from the ground displacement, rather than the inertial effects from the superstructure, when T_b was longer than T_g and the amplitude of δS was greater than that of δR. Under these circumstances, the restraint on the ground displacement by the grid-form DMWs could lead to significant decrease in bending moment of the piles.

REFERENCES

Hamada, J., Shigeno, Y., Onimaru, S., Tanikawa, T., Nakamura, N. and Yamashita, K. (2014): Numerical analysis on seismic response of piled raft foundation with ground improvement based on seismic observation records, *Proc. of the 14th Int. Assoc. Computer Methods and Recent Advances in Geomechanics*, 719-724.

Tamura, S., Fujimori, T., Shoji, M., Mimachi, T., Mano, H., Uchida, A., Funahara, H. and Sekiguchi, T. (2012): Reduction factors of soil displacement and inertia forces for seismic deformation method, *Summaries of Technical Papers of Annual Meeting, AIJ*, 519-520 (in Japanese).

Tamura, S. and Hida, T. (2014): Pile stress estimation based on seismic deformation method with embedment effects on pile caps, *J. Geotechnical and Geoenvironmental Engineering, ASCE*, Vol:140, No.9, 04014049.

Yamashita, K., Hamada, J., Onimaru, S. and Higashino, M. (2012): Seismic behavior of piled raft with ground improvement supporting a base-isolated building on soft ground in Tokyo, *Soils & Foundations*, Vol. 52 (5), 1000-1015.

Yamashita, K., Shigeno, Y., Hamada, J. and Chang, D. W. (2018): Seismic response analyses of piled raft with grid-form deep mixing walls under strong earthquakes with performance-based design concerns, *Soils & Foundations*, Vol. 58 (1), 65-84.